

Accurate ro-vibrational rest frequencies of DC₄H at infrared and millimetre wavelengths[★]

F. Tamassia¹, L. Bizzocchi², C. Degli Esposti³, L. Dore³, M. Di Lauro³, L. Fusina¹, M. Villa¹, and E. Canè¹

¹ Dipartimento di Chimica Fisica e Inorganica, Università di Bologna, Viale del Risorgimento 4, 40136 Bologna, Italy
e-mail: filippo.tamassia@unibo.it

² Centro de Astronomia e Astrofísica, Observatório Astronómico de Lisboa, Tapada da Ajuda, 1349-018 Lisboa, Portugal

³ Dipartimento di Chimica “G. Ciamician”, Università di Bologna, via F. Selmi 2, 40126 Bologna, Italy

Received 13 September 2012 / Accepted 2 November 2012

ABSTRACT

Context. Diacetylene, C₄H₂, has been identified in several astronomical environments through its infrared spectrum. In contrast, monodeuterated diacetylene (DC₄H) has not been detected in space so far owing to the low isotopic abundance of deuterated species but also to the rather poor laboratory spectroscopic characterisation of this molecule.

Aims. The aim of this work is to provide accurate spectroscopic parameters for DC₄H to achieve reliable predictions for both its spectra at millimetre and infrared wavelengths.

Methods. We studied the rotational spectrum of DC₄H in the range 85–615 GHz by millimetre-wave spectroscopy and the infrared spectrum below 1000 cm⁻¹ by high-resolution, Fourier-transform spectroscopy. Several pure rotational transitions were recorded in the ground state and in excited vibrational bending states. The three fundamental bands ν_6 , ν_7 , and ν_8 have been identified and assigned in the infrared spectrum.

Results. The rotational transitions were analysed together with the infrared data in a global fit that produces very accurate ro-vibrational parameters. The observed frequencies and wavenumbers are reported to provide precise guidance for astronomical searches.

Key words. ISM: molecules – line: identification – molecular data – molecular processes – infrared: ISM

1. Introduction

Many polyatomic molecules discovered in space are carbon chains with an acetylenic structure, i.e., featuring alternating single and triple C–C bonds. The simplest members of the family, acetylene (C₂H₂) and diacetylene (C₄H₂), play a major role in the synthesis of complex interstellar molecules: ion-neutral or neutral-neutral reactions between these moieties and C⁺ or CN lead to the production of larger hydrocarbons (C_mH_n) or cyanopolyynes (HC_{2n}CN) (Cherchneff & Glassgold 1993). Chain polymerisation then culminates in the formation of complex aliphatic and possibly aromatic structures that compose the solid carbon-based materials present in the interstellar medium (ISM, Frenklach & Feigelson 1989; Allamandola et al. 1989; Kwok 2009).

Despite their astrophysical relevance, C₂H₂ and C₄H₂ remain rather elusive for detection in the ISM due to the lack of electric permanent dipole moment and thus of pure rotational spectrum. As a result, they have only been observed in the infrared (IR). The main isotopic species of acetylene have been observed with high abundances in both cold (<100 K) and warm (100–1000 K) gas (e.g., Lacy et al. 1989; Evans et al. 1991; Carr et al. 1995; Lahuis & van Dishoeck 2000; Farrah et al. 2007; Sonnentrucker et al. 2007). Diacetylene has been

observed in the proto-planetary nebulae CRL 618 and CRL 2688 (Cernicharo et al. 2001), and also outside our galaxy in a similar object embedded in the Large Magellanic Cloud (SMP LMC 11, Bernard-Salas et al. 2006). However, the high $N(\text{C}_2\text{H}_2)/N(\text{C}_4\text{H}_2)$ column density ratio (~ 2) derived in CRL 618 (Cernicharo et al. 2001) suggests that substantial abundances of diacetylene may be present in the warm gas of many carbon-rich environments. C₄H₂ is also a well known constituent of the stratosphere of the giant planets and their moons (e.g., de Graauw et al. 1997; Fouchet et al. 2005; Coustenis et al. 2007). Very recently, the ¹³C isotopologue of diacetylene has been observed in Titan's spectra (Jolly et al. 2010). There, it acts as a UV shield and is thought to play a major role in the photochemical reactions originating the organic aerosols (tholines) present in the atmospheres of these solar system bodies (Waite et al. 2007).

Although the cosmic deuterium-to-hydrogen ratio is a few times 10⁻⁵, isotopic fractionation mechanisms in the ISM are able to produce large D-enhancement in many molecules, and deuterated isotopologues are indeed observed with relative abundances up to a few percent or more of their parent species (Herbst 2003).

In the gas phase, the deuterium fractionation is generally driven by exothermic ion-neutral reactions in low-temperature environments (e.g., Roberts & Millar 2000). However, experimental and theoretical investigations have shown that D-enrichments in complex hydrogen-deficient organic molecules can be achieved via a barrierless and exoergic neutral-neutral reaction involving the dicarbon radical C₂ in its

[★] Full Table 4 is only available in electronic form at the CDS via anonymous ftp to cdsarc.u-strasbg.fr (130.79.128.5) or via <http://cdsarc.u-strasbg.fr/viz-bin/qcat?J/A+A/549/A38>

$a^3\Pi_u$ electronic excited state (Guo et al. 2006). This process is enhanced at high temperatures and could sustain the production of deuterated carbon chains in the warm gas, for example, close to the photosphere of evolved carbon-rich stars.

Deuterated hydrocarbons are also important proxies for the D/H isotopic composition of planetary atmospheres, which in turn provide important information on the evolutionary models of the solar nebula (Coustenis et al. 2007, 2010). Mono-deuterated acetylene (DC_2H) has been recently detected in Titan by Cassini/CIRS yielding a D/H ratio that is significantly higher than those measured in methane (Coustenis et al. 2008). Diacetylene produces one of the strongest emission features of Titan below 1000 cm^{-1} (ν_6 , see, e.g. the CIRS limb spectrum shown in Bézard 2009), thus it is very likely that singly deuterated diacetylene (DC_4H) can also be identified, providing further insight into the origin of the Titan's atmosphere.

Clearly, D-bearing hydrocarbons are elusive species, and many of them have so far escaped detection owing to the lack of sufficiently reliable spectroscopic data. The laboratory spectroscopic characterisation of DC_4H is manifestly inadequate for astrophysical purposes.

Its IR spectrum has only been studied at high resolution at wavelengths shorter than $10\mu\text{m}$. The strong ν_1 fundamental at 3300 cm^{-1} and its overtones were investigated by Gambogi et al. (1995) using a molecular-beam laser spectrometer. The other intense ν_4 fundamental at 2600 cm^{-1} and some other combination bands at 1250 cm^{-1} were recorded by Tay et al. (1995) with a Fourier-transform infrared (FTIR) spectrometer. No high-resolution studies exist for the spectral region below 1000 cm^{-1} where the bending fundamentals ν_6 , ν_7 , and ν_8 are located. These bands, centred at 627 , 471 , and 499 cm^{-1} respectively, are the strongest features in the IR spectrum of diacetylene, so they provide the most viable means for astronomical detections. Only a low-resolution gas-phase spectrum is presently available in literature (Owen et al. 1987).

Noteworthy, DC_4H lacks the centre of symmetry because of the single D substitution. Thus it acquires a small permanent dipole moment in its ground vibrational state. This effect is strongly enhanced by molecular vibration in low-lying bending excited states (Matsumura & Tanaka 1986a,b), and creates a detectable pure rotational spectrum at millimetre (mm) wavelengths (Etoh et al. 1981), in which, at room temperature, the strongest features are due to the $\nu_6 = 1$ excited state.

Because the well known (e.g. IRC+10216, see Cernicharo et al. 2011) chemically rich regions have a high degree of vibrational excitation, it is likely that multiply excited vibrational states of diacetylene are also appreciably populated. With the forthcoming completion of the Atacama Large Millimetre Array (ALMA), there will be a major step toward sensitivity and spectral resolution; consequently, weak lines of numerous large polyatomic and rare-isotope molecules are likely to be detected. If DC_4H is present in the hot gas of circumstellar environments, the emission at millimetre wavelengths from the excited states of its ν_6 manifold (those with the largest induced dipole moment) can provide a precise tool for astronomical detections.

The pure rotational spectrum of DC_4H has already been identified in the laboratory by Etoh et al. (1981) and Tanaka et al. (1988). They recorded a few transitions in the microwave region for the ground state, as well as lines belonging to various excited states involving the ν_6 , ν_8 , and ν_9 bending vibrations. State-specific values of the vibrationally induced electric dipole moment were also estimated through Stark-effect and intensity measurements. More recently, ground-state low- J transitions of DC_4H have been reinvestigated at higher resolution by

Matsumura et al. (2006) in the 8–25 GHz frequency range using a Fourier transform microwave (FTMW) spectrometer, thereby determining the small deuterium, quadrupole coupling constant.

High-resolution FTIR measurements were performed in the $450\text{--}1000\text{ cm}^{-1}$ range, leading to the identification and analysis of the ν_6 , ν_7 , and ν_8 fundamental bands. Furthermore, we extended the investigation of the pure rotational spectra of the ground and of the singly excited bending states $\nu_6 = 1$, $\nu_8 = 1$, and $\nu_9 = 1$ to the sub millimetre (submm) region, covering the 85–615 GHz frequency interval and reaching a J quantum number as high as 74.

In this paper we present the results of a comprehensive new laboratory investigation of the ro-vibrational spectrum of DC_4H . Following what we have done in our previous papers on HC_4H (Bizzocchi et al. 2010, 2011), our main effort aims to provide state-of-the-art spectroscopic data on DC_4H to the astronomical community. These data are very useful for infrared and/or millimetre studies. The spectral analyses yielded the very accurate values of the spectroscopic constants needed to predict precise millimetre and IR rest frequencies for all the band and vibrational states investigated.

2. Experimental

The sample of DC_4H employed in this work was produced by the method described by Armitage et al. (1951), i.e. by reaction of 1,4-dichloro-2-butyne (Aldrich) with sodium hydroxide dissolved in a nearly equimolar mixture of H_2O and D_2O . The rotational spectra of DC_4H in the ground state and in the excited bending states have been recorded in selected frequency regions between 85 and 615 GHz, using the mm-wave spectrometer employed to record the $\nu_8 - \nu_6$ difference band for the symmetric isotopologues HC_4H and DC_4D (Bizzocchi et al. 2010). Briefly, the radiation sources were phase-locked Gunn oscillators (75–115 GHz range) equipped with various frequency multipliers, and the absorption cell was a 3 m long glass tube sealed by PTFE windows. Signal detection was performed using a liquid-helium-cooled InSb detector. Source frequency modulation was applied, and the signal was demodulated at $2f$, thus obtaining the second derivative of the actual spectrum profile. About 150 rotational transition frequencies of DC_4H have been measured, with experimental uncertainties of $\sim 30\text{ kHz}$. All the measurements were performed at room temperature, at a static pressure of $\sim 1.5\text{ Pa}$.

The infrared spectra were recorded with a Bomem DA3.002 Fourier-transform spectrometer equipped with a Global source, a KBr beamsplitter, and a liquid nitrogen-cooled HgCdTe detector. The attained resolution was either 0.004 or 0.006 cm^{-1} . Several spectra were recorded at pressures between 40 and 800 kPa. We mostly used a 0.18 m long absorption cell, but also a multipass White-type cell with an effective pathlength of 10 m was employed. Several hundred scans, up to 860, were co-added in order to improve the signal to noise ratio of the spectra. Ro-vibrational transitions of H_2O (Toth 1991) and CO_2 (Horneman 2007) were used for calibration. The average precision of our measurements was estimated to be around 0.0004 cm^{-1} .

3. Observed spectra and analysis

3.1. Millimetre-wave spectra

Previous recordings of a few rotational transitions ($\nu \leq 80\text{ GHz}$) for various low-lying vibrational states of DC_4H had

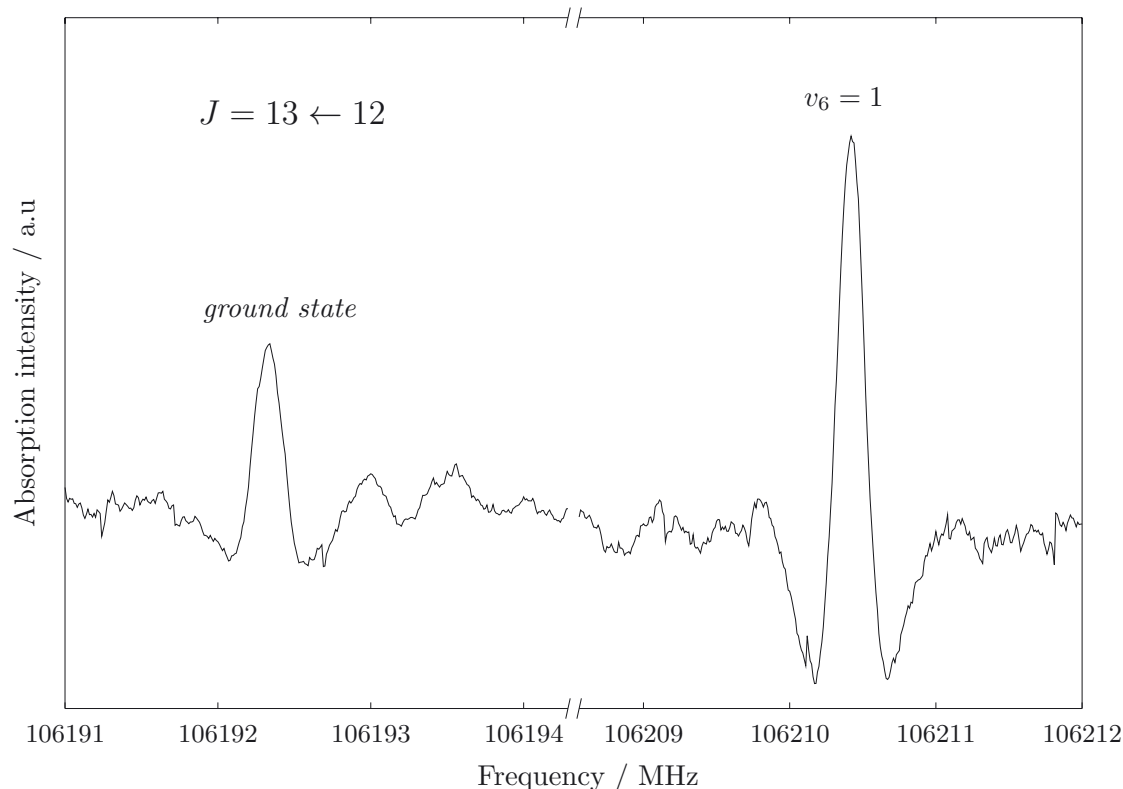


Fig. 1. Recording of the $J = 13 \leftarrow 12$ rotational transitions of DC₄H in the ground state (left trace) and $v_6 = 1$ excited state (right trace). Two short portions of a single longer scan are presented.

been already reported (Etoh et al. 1981; Tanaka et al. 1988; Matsumura et al. 2006). In the present work we have extended the measurements for the ground state and singly excited bending states $v_6 = 1$, $v_8 = 1$, and $v_9 = 1$ into the submm region, by observing *ca.* 150 pure rotational transitions with J ranging from 10 to 74. The assignment of the new lines was guided by the literature spectroscopic data, making use of the basic rotational energy level expression for linear polyatomic molecules, including the l -type doubling contribution where appropriate (e.g., see Eq. (5.25) in Gordy & Cook 1984). An example of the observed spectra showing ground and $v_6 = 1$ state transitions is given in Fig. 1. Due to the vibrationally enhanced dipole moment, the excited-state line is *ca.* 2.5 times more intense than the ground state line, despite the less favourable population factor.

3.2. Infrared spectra

No high-resolution investigation of the IR spectra of DC₄H below 1000 cm⁻¹ has ever been reported. We observed about 760 ro-vibrational transitions for the v_6 , v_7 , and v_8 fundamental bands. The infrared spectra were recorded at different pressures in order to have very accurate measurements even for the high- J transitions. The J values of the observed transitions are 1–117 for v_6 , 1–81 for v_7 , and 3–100 for v_8 . Besides the v_6 , v_7 , and v_8 fundamental bands, several hot bands have been identified and analysed and will be the subject of a future paper. Initially, the transition wavenumbers of each band were fitted separately, in order to check the correctness of the assignments and to extend the data set. The data were analysed using the basic ro-vibrational energy level expression of a linear molecule (Fusina et al. 2011) with centrifugal distortion corrections up to the sextic term. Since all these bands involve bending modes, the

l -type doubling energy contributions were included in the model. A portion of the recorded spectrum showing the v_6 fundamental and the associated hot band system is illustrated in Fig. 2.

3.3. Spectral analysis

Eventually, all mm-wave and infrared data were fitted simultaneously in a single least-squares procedure. A comprehensive summary of the relevant ro-vibrational theory, including the expression of the Hamiltonian matrix elements used in the present analysis is reported in Appendix A.

A proper weighting factor ($w_i = 1/\sigma_i^2$) was assigned to each data point, in order to take the different measurement precisions of the various data sets into account. The following σ_i values were used for the literature data: 1 kHz for the hyperfine-free, ground-state transition frequencies derived from the FTMW study of Matsumura et al. (2006); 20 kHz for the mm-wave lines of ground, $v_8 = 1$, and $v_9 = 1$ states (Tanaka et al. 1988); 50 kHz for the $v_6 = 1$ rotational frequencies reported by Etoh et al. (1981). For the data collected in the present investigation, we assumed a $\sigma_i = 20$ or 40 kHz for the lines below or above 420 GHz, respectively. Finally, $\sigma_i = 5 \times 10^{-4}$ cm⁻¹ was adopted for the present IR measurements.

The fit of the transitions of the $v_6 = 1$ bending state showed anomalous residuals. Considering that the $v_9 = 3$ state is only 3 cm⁻¹ apart, we postulated a quartic anharmonic resonance between these two states, which has been explicitly considered in our analysis. Generally speaking, to determine the interaction term (W_{6999} , see Eq. (A.3) in Appendix A), it is necessary to include experimental transitions involving both interacting states. Since we did not observe any transition belonging to $v_9 = 3$, we chose to fix its rotational parameters in the following

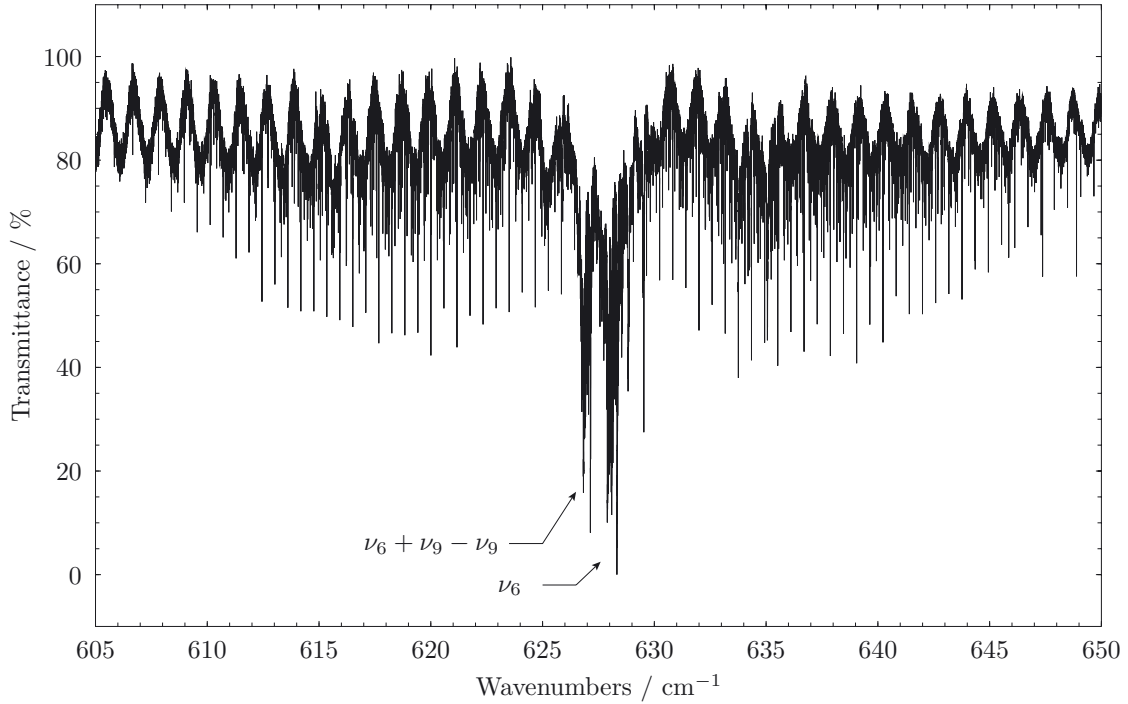


Fig. 2. Portion of the infrared spectrum of DC₄H showing the ν_6 band, centred at $\nu_0 = 626.9609 \text{ cm}^{-1}$. The hot band $\nu_6 + \nu_9 - \nu_9$ is also visible at $\nu_0 = 625.9136 \text{ cm}^{-1}$. Experimental conditions: pressure 67 Pa, absorption path length 0.18 m, resolution 0.004 cm^{-1} , 200 scans.

Table 1. Band origins and vibrational state constants for the unperturbed vibrational bands of DC₄H.

Parameter	Unit	Ground state <i>This work</i>	Ground state (Tanaka et al. 1988)	$\nu_7 = 1$
ν_0	/ cm^{-1}			471.401399(64)
B_v	/ MHz	4084.453438(68)	4084.4546(18)	4090.6191(19)
D_v	/ kHz	0.394107(29)	0.402(12)	0.40229(36)
H_v	/ mHz	0.0280(36)		0.0280 ^a
q_v	/ MHz			3.0402(22)
q_{vJ}	/ Hz			-3.56(54)

Notes. The numbers in parentheses are 1σ uncertainties expressed in units of the last quoted digit. ^(a) Fixed.

way: B_v and D_v were linearly extrapolated from the corresponding values of the ground and $\nu_9 = 1$ state, while the values of $\nu_9 = 1$ state were adopted for the other constants. Since the rotational transitions in $\nu_9 = 1$ are also included in the global fit, the parameters of $\nu_9 = 3$ were derived through an iterative procedure. The l -doubling constants q_v and q_{vJ} were held fixed to the values determined for $\nu_9 = 1$. The energy separation between the two states, $\Delta E = E_{\nu_9=3,l=1} - E_{\nu_9=1}$, was also adjusted iteratively.

The final data set, purged of perturbed spectral features and spurious measurements, comprises a total of 787 transitions. The overall weighted root mean square of the fit residuals is 0.795. The parameters derived from the least-squares procedure are listed in Tables 1–3. The fitted constants are all very well determined, and the comparison with previously available data (also reported in the Tables) shows improvements up to two orders of magnitude in precision. Including the precise mm-wave data in the data set was beneficial for significantly reducing the correlations between the lower- and upper- state parameters of the analysed IR bands. Indeed, the slightly lower precision of the

parameters of the $\nu_7 = 1$ state derives from the lack of pure rotational data for that state. This is because excitation of the ν_7 vibrational mode does not enhance the dipole moment, and the lower population prevents any observation of the corresponding rotational lines.

4. Discussion and conclusions

The set of spectroscopic constants we have derived is a remarkable improvement over the previous work (Etoh et al. 1981; Tanaka et al. 1988) because it allows calculation of a very reliable set of rest frequencies for the rotational (millimetre) and ro-vibrational (IR) transitions that involve the ground-state and most of the singly excited bending states.

We collected the complete set of measured line positions, along with a comprehensive listing of predictions calculated from the spectroscopic data of Tables 1–3. The list also includes the estimated uncertainty at the 1σ level of each transition as determined statistically by the least-squares fits (Albritton et al. 1976). This table is available in its entirety in a machine-readable

Table 2. Band origins and vibrational state constants for the unperturbed vibrational bands of DC₄H.

Parameter	Unit	$\nu_8 = 1$	$\nu_8 = 1$	$\nu_9 = 1$	$\nu_9 = 1$
		<i>This work</i>	(Tanaka et al. 1988)	<i>This work</i>	(Tanaka et al. 1988)
ν_0	/ cm ⁻¹	498.395521(30)		210 ^a	
B_v	/ MHz	4089.64590(17)	4089.6490(51)	4095.68839(19)	4095.6938(52)
D_v	/ kHz	0.395035(50)	0.413(30)	0.409462(60)	0.433(30)
H_v	/ mHz	0.0280 ^b		0.0280 ^b	
q_v	/ MHz	2.63072(34)	2.631(2)	5.56810(38)	5.568(2)
q_{vJ}	/ Hz	-0.746(99)		-10.88(12)	

Notes. The numbers in parentheses are 1σ uncertainties expressed in units of the last quoted digit. ^(a) Low-resolution IR value from Owen et al. (1987). ^(b) Fixed.

Table 3. Band origin and vibrational state constants for the perturbed ν_6 band of DC₄H.

Parameter	Unit	$\nu_6 = 1$	$\nu_6 = 1$	$\nu_9 = 3, l = 1$
		<i>This work</i>	(Etoh et al. 1981)	
ν_0	/ cm ⁻¹	626.960886(97)		
B_v	/ MHz	4086.17536(79)	4086.2165(44)	4118.1583 ^a
D_v	/ kHz	0.39449(12)	0.408(36)	0.4402 ^a
H_v	/ mHz	0.0400(75)		0.0280 ^a
q_v	/ MHz	2.11692(20)	2.1316(28)	5.56810 ^a
q_{vJ}	/ Hz	-0.538(44)		-10.88 ^a
W_{6999}	/ cm ⁻¹	0.10804(89)		
ΔE	/ cm ⁻¹	3.039114 ^a		

Notes. The numbers in parentheses are 1σ uncertainties expressed in units of the last quoted digit. ^(a) Assumed values, see text. $\Delta E = E_{\nu_9=3,l=1} - E_{\nu_6=1}$.

Table 4. Measured and predicted line positions of DC₄H.

J'	l'	p'	v'	J	l	p	v	RF_{meas}	RF_{pred}	1σ	Unit	$S_{J'J}$
27	0	e	0	26	0	e	0		220 529.4600	0.0033	MHz	27.000
28	0	e	0	27	0	e	0	228 694.807(20)	228 694.7903	0.0033	MHz	28.000
29	0	e	0	28	0	e	0		236 859.8559	0.0032	MHz	29.000
...												
27	1	e	6	26	1	e	6		220 566.5625	0.0032	MHz	26.916
27	1	f	6	26	1	f	6		220 681.0695	0.0033	MHz	26.921
28	1	e	6	27	1	e	6	22 8733.225(20)	228 733.2318	0.0032	MHz	27.917
28	1	f	6	27	1	f	6	228 851.958(20)	228 851.9597	0.0032	MHz	27.923
29	1	e	6	28	1	e	6	236 899.630(20)	236 899.6341	0.0031	MHz	28.918
...												
40	1	e	6	41	0	e	0	615.6900(5)	615.690049	3.4×10^{-5}	cm ⁻¹	19.988
39	1	e	6	40	0	e	0	615.9605(5)	615.960462	3.4×10^{-5}	cm ⁻¹	19.488
38	1	e	6	39	0	e	0	616.2310(5)	616.230932	3.4×10^{-5}	cm ⁻¹	18.988
37	1	e	6	38	0	e	0		616.501459	3.4×10^{-5}	cm ⁻¹	18.488
...												

Notes. For a detailed description see Sect. 4. This table is available in its entirety at the CDS. A portion is shown here to indicate its form and content.

form at the CDS. An excerpt is shown in Table 4, and it includes the following columns:

- (1–4) J', l', p', v' . Rotational, vibrational quantum numbers, and e/f parity of the upper level;
- (5–8) J, l, p, v . Rotational, vibrational quantum numbers, and e/f parity of the lower level;
- (9) RF_{meas} . Measured line position. The numbers in parentheses are the assumed experimental uncertainties expressed in units of the last quoted digit;
- (10) RF_{pred} . Predicted line position evaluated from the spectroscopic constants of Tables 1–3;
- (11) 1σ . Estimated error of the prediction at 1σ level;

- (12) unit. MHz or cm⁻¹;
- (13) $S_{J'J}$. Line strength.

The corresponding Einstein A-coefficients for spontaneous emission can then be calculated for each $J' \rightarrow J$ line using (Herzberg 1950)

$$A_{J'J} = \frac{16\pi^3}{3\epsilon_0 h c^3} \frac{\nu_{J'J}^3}{2J' + 1} S_{J'J} \mathfrak{R}^2, \quad (1)$$

where $\nu_{J'J}$ is the transition frequency (units of Hz), $S_{J'J}$ the line strength factor as given in Table 4, and \mathfrak{R}^2 the squared transition dipole moment (units of C² m²). For a purely rotational transition, $\mathfrak{R}^2 = \mu^2$, where μ is the permanent electric dipole moment.

For a vibration-rotation transition, the squared transition dipole moment is expressed as

$$\mathfrak{R}^2 = |R_{v'v}^0|^2 F, \quad (2)$$

where $|R_{v'v}^0|$ is the rotationless vibrational transition dipole moment, and F the product of the Herman-Wallis factors which, for linear molecules, are expressed as

$$F_{RP} = [1 + A_1 m + A_2^{RP} m^2]^2 \quad \text{for } P \text{ and } R \text{ branch lines,}$$

$$F_Q = [1 + A_2^Q J(J+1)]^2 \quad \text{for } Q \text{ branch lines,}$$

where $m = -J$ and $m = J + 1$ for the P and R branches, respectively.

In this work we have provided important spectroscopic information about the monodeuterated isotopologue of diacetylene. A number of rotational and ro-vibrational parameters were determined from a global fit of microwave and infrared data. The list of observed transitions, together with the line strength factors, can be a useful guide for astronomical searches of this molecule.

Acknowledgements. The authors acknowledge the Università di Bologna and the Ministero della Ricerca e dell'Università for financial support under the grant PRIN09 "High-resolution Spectroscopy for Atmospheric and Astrochemical Research: Experiment, Theory and Applications". L.B. gratefully acknowledges support from the Science and Technology Foundation (FCT, Portugal) through the Fellowship SFRH/BPD/62966/2009. The authors also thank Prof. G. Di Lonardo for helping record of the infrared spectra.

Appendix A: Theory

In the spectral analysis presented in this paper, each ro-vibrational energy term has been expressed with the formalism originally developed by Yamada and co-workers (Yamada et al. 1985; Niederhoff & Yamada 1993), and previously employed to fit the excited state rotational spectra of HC₅N (Yamada et al. 2004). Briefly, the ro-vibrational Hamiltonian is first represented using the symmetric top basis functions $|v, l, J, k\rangle$ (with $k = l$ for the states treated in the present paper), where v is a bending vibrational quantum number. The elements of the Hamiltonian matrix that are diagonal in the quantum numbers v and l are

$$\langle v, l, J, k | \hat{H} | v, l, J, k \rangle = G_v + B_v \{J(J+1) - k^2\} - D_v \{J(J+1) - k^2\}^2 + H_v \{J(J+1) - k^2\}^3, \quad (A.1)$$

where G_v is the "pure" vibrational energy of the $|v, l\rangle$ state and includes the appropriate anharmonic corrections. The origin of a ro-vibrational band, v_0 , is then given as $G'_v - G''_v$.

For excited bending vibrational states there is an l -type doubling contribution ($\Delta l, \pm 2, |\Delta k| = 2$) which has the general form:

$$\langle v, l \pm 2; J, k \pm 2 | \hat{H} | v, l, J, k \rangle = \frac{1}{4} \{q_t + q_{tJ} J(J+1)\} \times \sqrt{(v \mp l)(v \pm l + 2)} \times \sqrt{[J(J+1) - k(k \pm 1)][J(J+1) - (k \pm 1)(k \pm 2)]}; \quad (A.2)$$

The resulting energy matrix is factorised into symmetric and antisymmetric blocks by adopting Wang-type linear combinations of wave-functions (e.g., Yamada et al. 2004, Eq. (4)), thus any sublevel belonging to a given vibrational state can be labelled

through its k value and by the "+" or "-" subscripts, which designate the sign of the symmetrised linear combination or, alternatively, with the e, f parity labels (Brown et al. 1975) using the correspondence $- \leftrightarrow e, + \leftrightarrow f$, valid for k odd.

The fit of the transitions of the $v_6 = 1$ bending state showed anomalous residuals. Considering that the $v_9 = 3$ state is only 3 cm^{-1} apart, we postulated a quartic anharmonic resonance between these two states, which has been explicitly considered in our analysis. The $\Delta k = 0$ interaction term was included in the Hamiltonian, and the corresponding off-diagonal matrix elements in the symmetrised basis are expressed by (Okabayashi et al. 1999)

$$e, f \langle v_6 = 1, l = 1; J, 1 | \hat{H}_{40} | v_9 = 3, l = 1; J, 1 \rangle_{e, f} = W_{6999}. \quad (A.3)$$

References

- Albritton, D. L., Schmeltekopf, A. L., & Zare, R. N. 1976, *Molecular Spectroscopy: Modern Approach II* (New York: Academic Press), 1
- Allamandola, L. J., Tielens, A. G. G. M., & Barker, J. R. 1989, *ApJS*, 71, 733
- Armitage, J. B., Jones, R. H., & Whiting, M. C. 1951, *J. Chem. Soc.*, 44
- Bernard-Salas, J., Peeters, E., Sloan, G. C., et al. 2006, *ApJ*, 652, L29
- Bézar, B. 2009, *R. Soc. London Phil. Trans. A*, 367, 683
- Bizzocchi, L., Degli Esposti, C., & Dore, L. 2010, *Mol. Phys.*, 108, 2315
- Bizzocchi, L., Tamassia, F., Degli Esposti, C., et al. 2011, *Mol. Phys.*, 109, 2181
- Brown, J. M., Hougen, J. T., Huber, K.-P., et al. 1975, *J. Mol. Spectrosc.*, 55, 500
- Carr, J. S., Evans, II, N. J., Lacy, J. H., & Zhou, S. 1995, *ApJ*, 450, 667
- Cernicharo, J., Heras, A. M., Tielens, A. G. G. M., et al. 2001, *ApJ*, 546, L123
- Cernicharo, J., Agúndez, M., Kahane, C., et al. 2011, *A&A*, 529, L3
- Cherchneff, I., & Glassgold, A. E. 1993, *ApJ*, 419, L41
- Coustenis, A., Achterberg, R. K., Conrath, B. J., et al. 2007, *Icarus*, 189, 35
- Coustenis, A., Jennings, D. E., Jolly, A., et al. 2008, *Icarus*, 197, 539
- Coustenis, A., Jennings, D. E., Nixon, C. A., et al. 2010, *Icarus*, 207, 461
- de Graauw, T., Feuchtgruber, H., Bezar, B., et al. 1997, *A&A*, 321, L13
- Etoh, T., Matsumura, K., & Tanaka, T. 1981, *J. Mol. Spectrosc.*, 89, 511
- Evans, II, N. J., Lacy, J. H., & Carr, J. S. 1991, *ApJ*, 383, 674
- Farrah, D., Bernard-Salas, J., Spoon, H. W. W., et al. 2007, *ApJ*, 667, 149
- Fouchet, T., Bezar, B., & Encrenaz, T. 2005, *Space Sci. Rev.*, 119, 123
- Frenklach, M., & Feigelson, E. D. 1989, *ApJ*, 341, 372
- Fusina, L., Ospitali, F., Villa, M., & Tamassia, F. 2011, *Mol. Phys.*, 109, 257
- Gambogi, J. E., Pearson, R. Z., Yang, X., Lehmann, K. K., & Scoles, G. 1995, *Chem. Phys.*, 190, 191
- Gordy, W., & Cook, R. L. 1984, *Microwave molecular spectra* (New York: Wiley)
- Guo, Y., Kislov, V. V., Gu, X., et al. 2006, *ApJ*, 653, 1577
- Herbst, E. 2003, *Space Sci. Rev.*, 106, 293
- Herzberg, G. 1950, *Molecular spectra and molecular structure I. Spectra of diatomic molecules* (Malabar, FL, USA: Krieger)
- Horneman, V.-M. 2007, *J. Mol. Spectrosc.*, 241, 45
- Jolly, A., Fayt, A., Benilan, Y., et al. 2010, *ApJ*, 714, 852
- Kwok, S. 2009, *ApJS*, 319, 5
- Lacy, J. H., Evans, II, N. J., Achtermann, J. M., et al. 1989, *ApJ*, 342, L43
- Lahuis, F., & van Dishoeck, E. F. 2000, *A&A*, 355, 699
- Matsumura, K., & Tanaka, T. 1986a, *J. Mol. Spectrosc.*, 116, 320
- Matsumura, K., & Tanaka, T. 1986b, *J. Mol. Spectrosc.*, 116, 334
- Matsumura, K., Suenram, R. D., Lovas, F. J., & Tanaka, T. 2006, *J. Mol. Spectrosc.*, 240, 120
- Niederhoff, M., & Yamada, K. M. T. 1993, *J. Mol. Spectrosc.*, 157, 182
- Okabayashi, T., Tanaka, K., & Tanaka, T. 1999, *J. Mol. Spectrosc.*, 195, 22
- Owen, N. L., Smith, C. H., & Williams, G. A. 1987, *J. Mol. Struct.*, 161, 33
- Roberts, H., & Millar, T. J. 2000, *A&A*, 361, 388
- Sonnentrucker, P., González-Alfonso, E., & Neufeld, D. A. 2007, *ApJ*, 671, L37
- Tanaka, K., Kato, K., & Tanaka, T. 1988, *J. Mol. Spectrosc.*, 131, 272
- Tay, R., Metha, G. F., Shanks, F., & McNaughton, D. 1995, *Struct. Chem.*, 6, 47
- Toth, R. A. 1991, *J. Opt. Soc. Am. B*, 8, 2236
- Waite, J. H., Young, D. T., Cravens, T. E., et al. 2007, *Science*, 316, 870
- Yamada, K. M. T., Birss, F. W., & Aliev, M. R. 1985, *J. Mol. Spectrosc.*, 112, 347
- Yamada, K. M. T., Degli Esposti, C., Botschwina, P., et al. 2004, *A&A*, 425, 767